Kovove Mater. 48 2010 379–385
DOI: 10.4149/km_2010_6_379

Characterization of carbon nanofibers by SEM, TEM, ESCA and Raman spectroscopy

V. Puchý[1], P. Tatarko[1]*, J. Dusza[1], J. Morgiel[2], Z. Bastl[3], J. Mihály[4]

[1] *Institute of Materials Research, Slovak Academy of Sciences, Watsonova 47, 040 01 Košice, Slovak Republic*
[2] *Institute of Metallurgy and Materials Science of the Polish Academy of Sciences, Reymonta 25, 30 059 Krakow, Poland*
[3] *J. Heyrovský Institute of Physical Chemistry, Academy of Sciences of the Czech Republic, Dolejškova 3, 182 23 Prague 8, Czech Republic*
[4] *Chemical Research Center, Hungarian Academy of Sciences, Pusztaszeri út 59-67, H-1025 Budapest, Hungary*

Received 16 March 2010, received in revised form 29 June 2010, accepted 16 August 2010

Abstract

Carbon micro/nanofibers prepared by catalytic chemical vapor deposition have been characterized using scanning electron microscopy, transmission electron microscopy, high resolution electron microscopy, electron spectroscopy for chemical analysis and Raman spectroscopy. The outer diameter of the fibers varied from 50 nm to 600 nm with an average diameter of 120 nm, length from several micrometers to several tens of micrometers and inner diameters from 20 nm to 230 nm. Two types of fibers have been identified: cylindrical and bamboo-shaped. The cylindrical fibers are usually defect-free and consist of distinct graphite layers parallel to the fiber axes. The bamboo-shaped fibers often contain defects at the nano-level, their walls are built from domains with different orientations of graphite layers.

K e y w o r d s: carbon micro/nanofiber, cylindrical fiber, bamboo-shaped fiber

1. Introduction

In recent years, the research in the field of filamentous carbons has been focused on the development of carbon nanotubes (CNTs) with desirable morphology, optimized properties and with reduced cost of production [1–6]. Beside the CNTs, other filamentous carbons have also been developed as well, e.g. nanofibers [7–11]. Carbon nanotubes are usually referred to as highly graphitic structures with an orientation of the basal carbon planes parallel to the tube axes, and carbon nanofibers are structures with other orientation of the graphic lamella that results in a smaller or no central channel [11]. Carbon nanofibers (CNFs) are cylindrical or conical structures that have diameters varying from a few to hundreds of nanometers and lengths ranging from less than a micron to millimeters. The internal structure of carbon nanofibers varies and is comprised of different arrangements of modified graphene sheets. The main distinguishing characteristic of nanofibers from nanotubes is the stacking of graphene sheets of varying shapes [12].

Carbon nanofibers are often synthesized by chemical-vapor deposition, metal-catalyzed decomposition of hydrocarbons, hot filament-assisted sputtering, etc. [13, 14]. According to their processing route (composition of catalyst, synthesis temperature, reaction gas, etc.), the CNT exhibit different morphology and different arrangement of their graphene layers [15].

This outstanding graphitic structure is inherent in carbon nanofibers and enables their utilization as mechanical, electrical or/and thermal reinforcement elements in different composite materials. They can also be used at field emission peaks in monitor applications, as catalyst supports, or as electrode material in batteries [16]. According to the results minimal amounts of CNFs are highly suitable for utilization as functional filling materials, i.e. in polymers; especially in thermoplasts and duroplasts, carbon nanofibers are applied today to meet the requirements of present and future applications. For the above-mentioned applications there is essential to know the characteristics of CNTs and CNFs because their micro/nanostructure including surface characteristics plays a critical role

*Corresponding author: tel.: +421 55 7922457; fax: +421 55 7922408; e-mail address: ptatarko@imr.saske.sk

in the properties of composites in which they are reinforcing or functionalizing elements.

Different techniques/methods have been used for the characterization of CNTs and CNFs during the last decade, included scanning electron microscopy (SEM), transmission electron microscopy (TEM), high resolution transmission electron microscopy (HRTEM), electron spectroscopy for chemical analysis (ESCA), Raman spectroscopy, X-ray photoelectron spectroscopy, etc. [17–28].

The aim of the present contribution is to characterize carbon micro/nanofibers using different characterization techniques/methods in order to obtain information necessary for their application as additives to ceramics to improve their functional and mechanical properties.

2. Experimental material and methods

The experimental material was prepared by catalytic chemical vapor deposition (CCVD), which is equivalent to catalytic deposition from the gaseous phase (Electrovac AG) and supplied for the analysis by EMPA, Switzerland.

Field emission SEM (JEOL 7000F) was used for examination of the length, diameter and morphology of the carbon nanofibers. TEM and HRTEM were employed to observe the crystal structure and graphite layer arrangement. The TEM specimens were prepared by dispersing the CNF in acetone ultrasonic bath and dropping a suspension onto a carbon lace Cu grid. The TEM images and selected area electron diffraction patterns were recorded using an accelerating voltage of 200 kV.

In order to provide an information on chemical composition and carbon bonding the sample was examined by XPS and XAES methods using a VG ESCA3 MkII electron spectrometer. The spectra were recorded with Al Kα radiation and an electrostatic hemispherical analyzer operated in the fixed analyzer transmission mode. Detailed spectral scans were taken over C (1s), O (1s) and C KLL regions. The sample was conducting and static charging was not observed. Quantification of oxygen concentration was accomplished by correcting the photoelectron peak intensities for their cross-sections [29] and accounting for the dependence of the inelastic mean free path of photoelectrons on their kinetic energy [30]. Curve fitting of overlapping O (1s) lines was carried out using the lines of the Gaussian-Lorentzian shape.

Raman measurements were performed by a BioRad (Digilab) FT-Raman spectrometer using an excitation with 1064 nm radiation from a Nd:YAG laser at 200 mW. To reduce thermal emission during spectra acquisition and to gain acceptable quality Raman spectra, the samples were mixed and ground with spectroscopic grade potassium bromide (KBr). Spectra were recorded at 4 cm^{-1} resolution with white light correction by co-addition of 2048 individual spectra. The investigated sample area is approx. 2 mm, the estimated penetration depth for carbon materials (optically opaque) is around few tens nm [31]. For data manipulation, Grams/32 (Galactic Industries Corporation) software package was used, band positions were analyzed using a mixed Gaussian-Lorentzian curve-fitting procedure.

3. Results and discussion

The morphology of the carbon nanofibers is illustrated in Figs. 1 and 3. The SEM images reveal that the CNFs are typically cylindrical with an outer diameter of 50–250 nm and inner diameter from 20 nm to 230 nm. According to the SEM observation, the

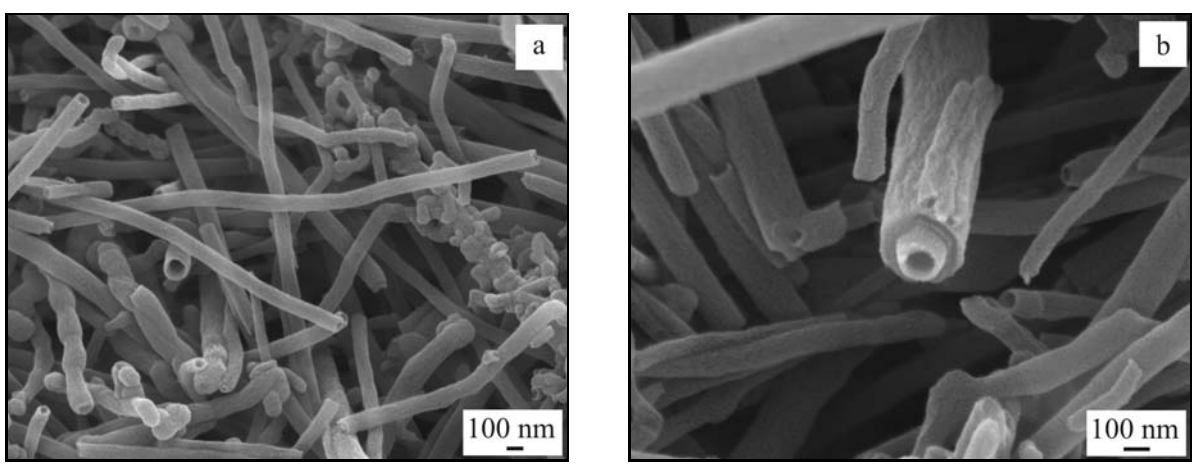

Fig. 1. Morphology of the carbon nanofibers, characteristic morphology with mix of cylindrical and bamboo-shaped nanofibers (a), an example for smooth CNF of small diameter and rough CNF of large diameter (b), SEM.

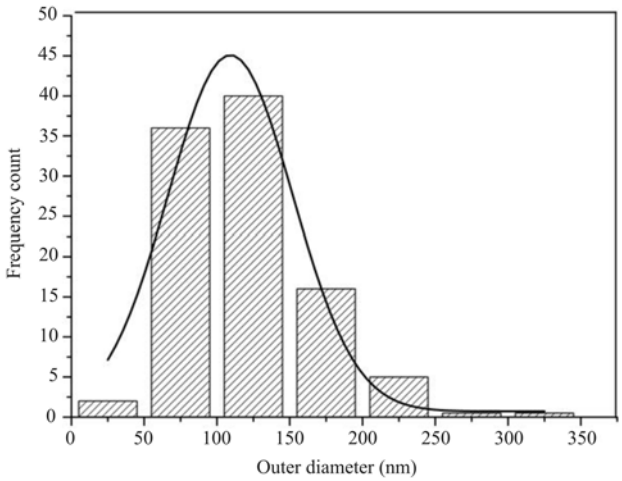

Fig. 2. Histogram illustrating the distribution of the diameters of the fibers.

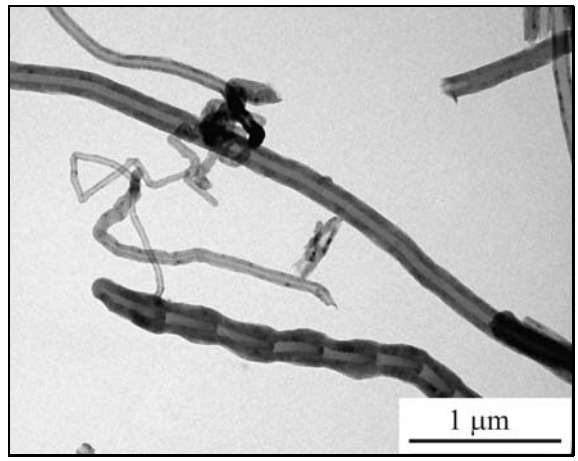

Fig. 3. Characteristic morphology of CNFs by TEM, cylindrical and bamboo-like CNFs.

length of the CNFs is up to several micrometers. In several cases we found clusters of the fibers with crooked and entangled fibers as well. Apart from the elongated carbon nanofibers, occasionally particle shaped carbon objects with a maximal size of several microns have also been identified. Two basic types of nanofibers have been identified by SEM observation: cylindrical hollow tubes, usually with free ends and smooth surface, and bamboo-shaped nanofibers with a waved surface. The third type of nanofibers with a straight-line shape and rough surface was identified only randomly. An observation of the end of the rope--fibers revealed that the diameter of the hole in the fiber was different and the wall of the fibers consisted of layers with different structure, Fig. 1b.

The study of the surface morphology of the fibers revealed that the fibers with smaller diameters were smoother compared to the fibers with larger diameters. Lee et al. [32] investigated the surface morphology of hollow and solid as-received, heat-treated and CVD surface treated fibers and found that the solid fibers exhibited a rougher surface compared to the hollow fibers in all forms. Measurement and statistical evaluation of the distribution of the diameters of nanofibers show their diameter changing from 50 to 600 nm with the average diameter equal to 120 nm, Fig. 2.

Results of TEM are in a good agreement with the results of SEM and it can be seen that in the case of cylindrical hollow fibers the wall is smooth and uniform and consists of a distinct sandwich of graphite layers. In this case the graphite layers are parallel to the axes of the fibers and forming usually defect-free material. The bamboo-shaped fibers are composed of multi-walled graphite structure and the bamboo sections have a size parallel with the axes of the fibers 2–3 times larger compared to the outer diameter of the fibers. It seems that the carbon diffusion was not continuous with all fibers during their growth, leading to a pulsed growth which translated into a periodic variation of the fiber diameter, as is illustrated in Fig. 3. Such bamboo-shaped fibers are composed of hollow segments of a size approximately 100 nm deliminated by curved stacking of carbon sheets, Fig. 3. Longtin et al. [31] prepared bamboo-type nanofibers by laser--assisted catalytic vapor deposition, applying two different catalyst preparation methods and the nanofibers analyzed using SEM, HREM and Raman spectroscopy. Using an approximately 50 nm thick deposited catalyst layer within the pores of an alumina substrate resulted in an array of vertically aligned nanofibers with similar dimension as the analyzed nanofibers in the present work. The lattice fringe analysis of HREM indicated that pulsed growth at high rates led to bamboo-type nanofibers having oriented graphitic domains, similarly as in our case. Bamboo-shaped carbon-nitrogen nanotubes were prepared by Lee [33] and Wu [34] using pyrolysis of iron pentacarbonyl and acetylene mixture with ammonia, and by pyrolysis of melamine with NaN_3-Fe-Ni and Ni catalyst, respectively. According to the results of Lee et al. [33], the nitrogen doping led to the origin of the bamboo--like structure and resulted in the degraded crystallinity of graphite sheets. By TEM they found that in the bamboo-like CN nanotubes the wall thickness increased due to the generation of compartment layers, but the outer diameter remained constant. This is different compared to the bamboo-like carbon nanotubes characterized in the present investigation, when the outer diameter of the nanofibers increased during the generation of compartment layers due to the changed orientation of the graphite sheets.

The internal structure of the fibers as related to the orientation of the graphite sheets is illustrated in Figs. 4–6. The fiber illustrated in Fig. 4 has a wall

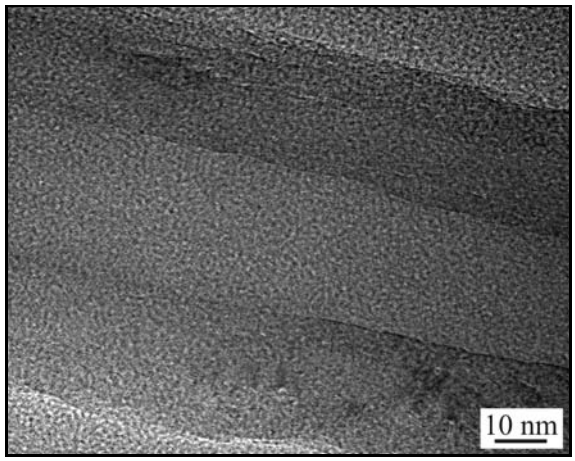

Fig. 4. HRTEM of a cylindrical nanofiber with the wall thickness of approximately 28 nm and hole diameter of approximately 30 nm. The interlayer spacing of the graphite layers is approximately 0.35 nm.

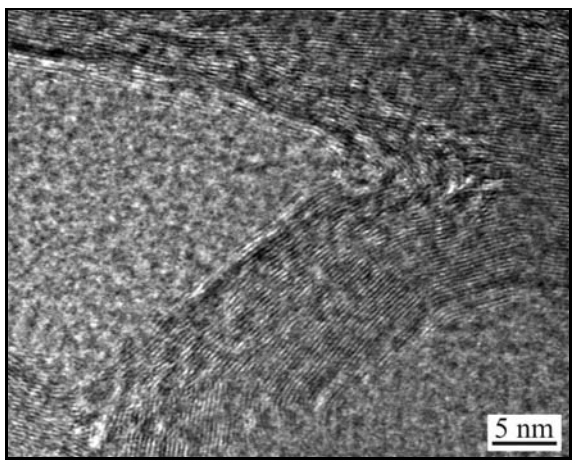

Fig. 5. HRTEM of a bamboo-shaped nanofiber with the wall thickness of approximately 18 nm. The interlayer spacing of the graphite layers in this wall is approximately 0.33 nm.

thickness of 28 nm and a hole diameter of 30 nm.

HRTEM reveals that the graphite structure of the wall parallel to the axes in some cases is similar to the pipe-shaped fibers, but sometimes these fibers consist of a wall from areas with differently oriented graphite layers. In Fig. 6 there is an example for a fiber with a wall, which consists of three areas (inner, middle and outer) with a graphite layer parallel to the axes (inner and outer) and having 22–34 degrees with the axes of the fiber. Similar characteristics were reported by Uchida et al. [13] and Lee et al. [32]. Uchida et al. [13] investigated the microstructure of a fiber heat treated at 3000 ℃ and found that the wall of the fiber consisted of two layers in which the individual graphite layers had different orientation to the axis of the fiber.

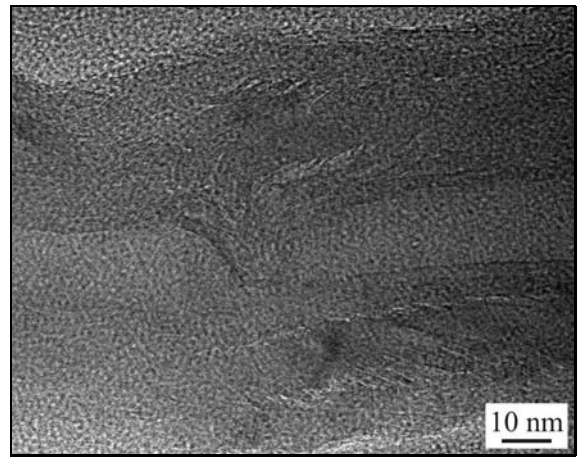

Fig. 6. HRTEM of a bamboo-shaped nanofiber with the main wall thickness of approximately 33 nm and connection wall thickness of approximately 13 nm. The main wall consists from inner, middle and outer areas with thickness of 8 nm, 33 nm and 10 nm, respectively. The interlayer spacing of the graphite layers in the middle area of the main wall is approximately 0.34 nm.

The graphite sheets of the inner layer varied between 4° and 36°, while in the outer layer they were oriented along the fiber axis. Lee et al. [32] found similar morphology in hollow fibers, which were heat treated at 2200 ℃, which exhibited two layers with different orientation of individual graphite sheets. They observed loops at both walls of the inner layer and found significant discontinuity between the inner and outer layers. Similar results were presented by Endo et al. [35] who investigated the internal structure of carbon nanofibers after heat treatment at temperatures from 1800 to 2100 ℃ by HRTEM. They found that some edge graphite planes were formed in single or multi loops whereas some end planes were strongly undulated. The graphite sheet arrangement and the formation of loops in carbon nanotubes and nanofibers were investigated by other authors as well [33–36]. Bamboo-shaped CNT and herringbone CNF have been catalytically synthesized by a decomposition of methane over Ni/Al catalyst under N_2 at temperatures from 500 to 600 ℃ by Zhao et al. [36]. They found two different bamboo-shaped tubes with different morphologies and structures.

The results of the ESCA analysis are illustrated in Fig. 7. Survey spectra revealed the presence of carbon and a small amount of oxygen. The O/C atomic concentration ratio calculated from integrated intensities of O (1s) and C (1s) photoemission lines was equal to 0.01. According to the results, the analyzed carbon nanotubes consist of 99.05 at.% carbon and 0.05 at.% oxygen. The binding energy of O (1s) electrons, 532.7 eV corresponded to carbon in C–O bonds.

The spectrum of C (ls) photoelectrons did not dif-

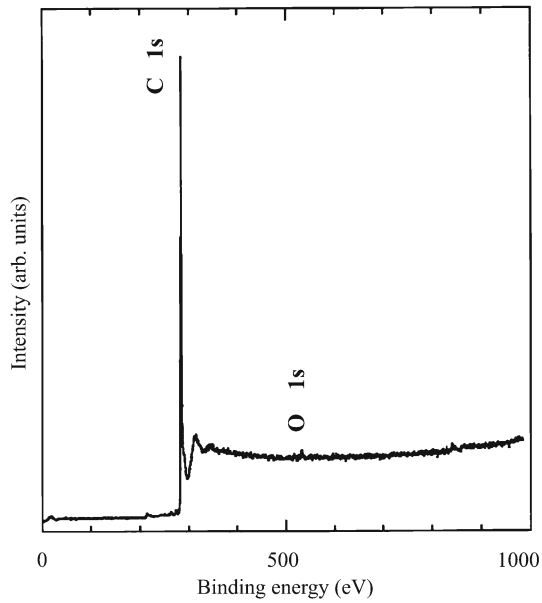

Fig. 7. Survey spectra measured in the interval of 0–1000 eV.

fer significantly from that of graphite; it exhibited asymmetric tailing towards higher binding energies, and weak plasmon satellite 6–7 eV apart from the parent C (ls) line, both pointing to the presence of carbon atoms with sp^2-like bonding symmetry [37–39].

A linear relationship between this separation and the sp^3/sp^2 ratio has been reported [40, 41]. The separation obtained for graphite, 22.3 eV agrees well with the data reported in the literature [40, 42]. For the studied sample we obtained the separation 19.4 eV, which corresponded to about 15 % of sp^3 hybridized C atoms.

Boudou et al. [43] characterized an as-received and surface treated isotropic carbon fiber by XPS and found rather modest structural changes induced by plasma treatment. The results of untreated sample were very similar to the results of the present investigation, but the atomic O/C ratio of 0.04 was slightly higher compared to the value of our experiment (0.01).

The result of Raman scattering in the 1800–1000 cm^{-1} wave number region is presented in Fig. 8. The spectrum is dominated by the two characteristic first-order Raman bands of carbonaceous materials: the so called *G-band* at 1600 cm^{-1} (E_{2g} mode of graphitic layers, produced from the high degree of carbon materials and generally used to identify well-ordered CNTs) and the *D-band* at 1282 cm^{-1} (disorder-induced phonon mode, related to disordered structures in carbon materials) [43]. The additional two weak noisy bands observed at around 1150 and 1370 cm^{-1} can be assigned to the mixed bonds between sp^2- and sp^3-carbon [44–46] and to semi-circle breathing mode of smaller aromatic ring systems [47], both typical for amorphous carbon structures.

Wave numbers (ν), full-widths at half-maximum (FWHM) and relative integrated intensity ratio (I_D/I_G) of the D-band and G-band obtained after a mixed Gaussian-Lorentzian deconvolution procedure are presented in Table 1.

Zang et al. [48] recently studied the characteristics of as-received and graphitized vapor-grown carbon nanofibers with the outer diameter similar as in the present study by Raman spectroscopy at excitation wavelength of 632.8 nm. They found that the first order Raman spectrum was composed of two main peaks, around 1340 cm^{-1} and 1590 cm^{-1} for the non-graphitized and 1340 cm^{-1} and 1582 cm^{-1} for graphitized nanofibers, respectively. The ratio of the intensity of D-band to G-band was 0.8 for non-graphitized

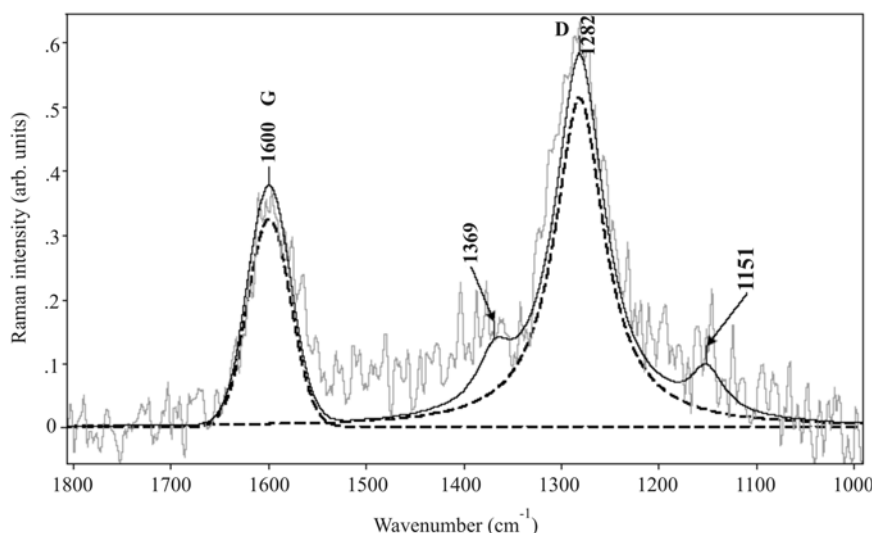

Fig. 8. Raman spectra of carbon nanofibers at 1064 nm excitation wavelength.

Table 1. Wavenumbers (ν), full-widths at half-maximum (FWHM) and relative intensity ratio of the D-band to the G-band (I_D/I_G) measured on the CNF

Sample	G-band (ν/cm^{-1})	G-band (FWHM/cm^{-1})	D-band (ν/ cm^{-1})	D-band (FWHM/cm^{-1})	I_D/I_G
CNF	1597	49.6	1283	57.8	1.69

and 0.37 for graphitized carbon nanofibers.

An increase in relative intensity of the D-band (and consequently also the I_D/I_G value) with near-infrared excitation (1064 nm), however, is common and is related to a larger electron-phonon interaction for D-band with respect to G-band. Antunes et al. [28] studied the Raman spectra of CNTs, carbon fiber, powder graphite and highly ordered pyrolithic graphite (HOPG). They used three Raman spectrometers with different excitation wavelengths of 514.5 nm, 785 nm and 1064 nm. Their results show that the D-band downshifts with increasing wavelength and its relative intensity increases. The G-band has its position nearly independent of excitation wavelengths. The relative intensities of the D and G bands (I_D/I_G) changed from approximately 0.4 to 5.7. At all excitation wavelengths the I_D/I_G was the highest for CNT with lowest external diameter and for all investigated materials the I_D/I_G was the highest at the excitation wavelength of 1064 nm.

As regards the position of the G and D bands, our results are in good agreement with the results of Antunes [28], Choi [49] and Park [50]. Choi and co-workers [49] studied structural characteristics of nanostructured carbon films prepared by the hot-filament chemical-vapor-deposition (HFCVD). They suggested the second-order Raman spectra measured with NIR excitation (1064 nm) as a suitable probing tool for good quality graphene sheets in nanosized carbon materials. They established that with shortening of the well-stacked graphene sheets and/or with degradation of wall quality the overtones and combination bands became very weak and broad, hard to distinguish. The fact that in our case no well-defined second-order Raman features were detected can be related to reducing the lateral size of flat and well-stacked graphene sheets (less than 25 nm) [51]. These observations are in good agreement with the TEM and SEM results regarding the bamboo-shaped fibers with characteristic bamboo segments.

4. Conclusions

Different techniques/methods were used for the characterization of carbon micro/nanofibers prepared by catalytic chemical vapor deposition.

The outer diameter of the fibers varied from 50 nm to 600 nm and the length of the fibers changed from several micrometers to several tens of micrometers. Two types of fibers have been identified; cylindrical and bamboo-shaped fibers. The cylindrical fibers are usually defect-free and consist of a distinct graphite layers parallel to the fiber axes. The bamboo-shaped fibers often contain defects at the nano-level, their walls are built from domains with a different orientation of graphite layers. The fibers contain 99.05 at.% carbon and 0.95 at.% oxygen with a binding energy of O (1s) electrons of 532.7 eV, which corresponds to carbon in C-O bonds. In the first-order Raman spectra, the positions of the G-band at 1600 cm^{-1} and D-band at 1282 cm^{-1} are very similar to the positions of the same bands for carbon fibers and different carbon nanotubes, recently tested at excitation wavelength of 1064 nm. The unresolved second-order Raman feature suggests the shortening of well-stacked graphene sheets and the presence of heavily detected regions. These establishments are in good agreement with TEM and SEM observations.

Acknowledgements

The work was supported by the Slovak Grant Agency project No. 2/4173/04, 2/7171/27, APVT-51-049702, APVV-0171-06, APVV-COST-0042-06, LPP-0203-07, LPP-0174-07, Centrum of Excellence NANOSMART and EC 6FP projects NENAMAT and KMM-NoE. The authors thank P. Švec for helpful discussion.

References

[1] IIJIMA, S.: Nature, *354*, 1991, p. 56.
[2] EBBESEN, T. W.—AJAYAN, P. M.: Nature, 358, 1992, p. 220. doi:10.1038/358220a0
[3] GUO, T.—NIKOLAEV, P.—THESS, A.—COLBERT, D. T.—SMALLEY, R. E.: Chem. Phys. Lett., *243*, 1995, p. 49. doi:10.1016/0009-2614(95)00825-O
[4] COUTEAU, E.—HERNADI, K.—SEO, J. W.—THIEN-NGA, L.—MIKÓ, C.—GAÁL, R.—FORRÓ, L.: Chem. Phys. Lett., *378*, 2003, p. 9. doi:10.1016/S0009-2614(03)01218-1
[5] HAFNER, J. H.—CHEUNG, C. L.—LIEBER, C. M.: J. Am. Chem. Soc., *121*, 1999, p. 9750. doi:10.1021/ja992761b
[6] TAKENAKA, S.—KOBAYASHI, S.—OGIHARA, H.—OTSUKA, K.: J. Catal., *217*, 2003, p. 79.
[7] HE, C. N.—ZHAO, N. Q.—DU, X. W.—SHI, C. S.—LI, J. J.—HE, F.: Mater. Sci. Eng., *479*, 2008, p. 248. doi:10.1016/j.msea.2007.06.048

[8] SOMANI, S. P.—SOMANI, P. R.—TANEMURA, M.—LAU, S. P.—UMENO, M.: Curr. Appl. Phys., *9*, 2009, p. 144. doi:10.1016/j.cap.2008.01.002
[9] ZOU, G.—ZHANG, D.—DONG, CH.—LI, H.—XIONG, K.—FEI, L.—QIAN, Y: Carbon, *44*, 2006, p. 828. doi:10.1016/j.carbon.2005.10.035
[10] ZHENG, J. S.—ZHANG, X. S.—LI, P.—ZHOU, X. G.—YUAN, W. K.: Catalysis Today, *131*, 2008, p. 270. doi:10.1016/j.cattod.2007.10.104
[11] VANDER WAL, R. L.—TICICH, T. M.—CURTIS, V. E.: Carbon, *39*, 2001, p. 2277. doi:10.1016/S0008-6223(01)00047-1
[12] MELECHKO, A. V.—MERKULOV, V. I.—MCKNIGHT, T. E.—GUILLORN, M. A.—KLEIN, K. L.—LOWNDES, D. H.—SIMPSON, M. L.: J. Appl. Phys., *97*, 2005, p. 041301.
[13] UCHIDA, T.—ANDERSON, D. P.—MINUS, M. L.—KUMAR, S.: J. Mater. Sci., *41*, 2006, p. 5851. doi:10.1007/s10853-006-0324-0
[14] CHAI, S. P.—ZEIN, S. H. S.—MOHAMED, A. R.: Diam. Rel. Mater., *16*, 2007, p. 1656. doi:10.1016/j.diamond.2007.02.011
[15] EBBESEN, T. W. (Ed.): Carbon Nanotubes: Preparation and Properties. Boca Raton, CRC Press 1997.
[16] DE JONG, K. P.—GEUS, J. W.: Catal. Rev.-Sci. Eng., *42*, 2000, p. 481. doi:10.1081/CR-100101954
[17] MERKOCI, A.: Microchim Acta, *152*, 2006, p. 157. doi:10.1007/s00604-005-0439-z
[18] YAO, N.—WANG, Z. L. (Eds.): Handbook of Microscopy for Nanotechnology. New York, Kluwer Academic Publishers 2005.
[19] HASSANIEN, A.—TOKUMOTO, M.: Carbon, *42*, 2004, p. 2649. doi:10.1016/j.carbon.2004.06.009
[20] BURIAN, A.—KOLOCZEK, J.—DORE, J. C.—HANNON, A. C.—NAGY, J. B.—FONSECA, A.: Diam. Relat. Mater., *13*, 2004, p. 1261. doi:10.1016/j.diamond.2003.10.050
[21] CAO, A.—XU, C.—LIANG, J.—WU, D.—WEI, B.: Chem. Phys. Lett., *344*, 2001, p. 13. doi:10.1016/S0009-2614(01)00671-6
[22] COWLEY, J.—SUNDELL, F.: Ultramicroscopy, *68*, 1997, p. 1. doi:10.1016/S0304-3991(97)00009-0
[23] DROPPA, R.—HAMMER, P.—CARVALHO, A. C. M.—DOS SANTOS, M.—ALVAREZ, F.: Non-Cryst. Solids, *299–302*, 2002, p. 874.
[24] LEE, Y. S.—CHO, T. H.—LEE, B. K.—RHO, J. S.—AN, K. H.—LEE, Y. H.: J. Fluorine Chem., *120*, 2003, p. 99. doi:10.1016/S0022-1139(02)00316-0
[25] JUNG, D. H.—KO, Y. K.—JUNG, H. T.: Mater. Sci. Eng., *24*, 2004, p. 117. doi:10.1016/j.msec.2003.09.006
[26] PEREIRA, M. F. R.—FIGUEIREDO, J. L.—ORFAO, J. J. M.—SERP, P.—KALCK, P.—KIHN, Y.: Carbon, *42*, 2004, p. 2807. doi:10.1016/j.carbon.2004.06.025
[27] AREPALLI, S.—NIKOLAEV, P.—GORELIK, O.—HADJIEV, V. G.—HOLMES, W.—FILES, B. et al.: Carbon, *42*, 2004, p. 1783.
[28] ANTUNES, E. F.—LOBO, A. O.—CORAT, E. J.—TRAVA-AIROLDI, V. J.— MERTIN, A. A.—VERÍSSIMO, C.: Carbon, *44*, 2006, p. 2202. doi:10.1016/j.carbon.2006.03.003
[29] SCOFIELD, J. H.: J. Electron Spectrosc. Relat. Phenom., *8*, 1976, p. 129. doi:10.1016/0368-2048(76)80015-1
[30] NIST Electron inelastic-mean-free-paths. Database ver. 1.1, NIST Gaithersburg, MD 20899, 2000.
[31] LONGTIN, R.—CARIGNAN, L. P.—FAUTEUX, C.—THERRIAULT, P.—PEGNA, J.: Diamond Relat. Mater., *16*, 2007, p. 1541. doi:10.1016/j.diamond.2006.12.055
[32] LEE, S.—KIM, T. R.—OGALE, A. A.—KIM, M. S.: Synth. Met., *157*, 2007, p. 644. doi:10.1016/j.synthmet.2007.07.005
[33] LEE, C. J.—LYU, S. C.—KIM, H. W.—LEE, J. H.—CHO, K. I.: Chem. Phys. Letters, *359*, 2002, p. 115.
[34] WU, X.—TAO, Y.—LU, Y.—DONG, L.—HU, Z.: Diam. Rel. Mater., *15*, 2006, p. 164. doi:10.1016/j.diamond.2005.09.018
[35] ENDO, M.—KIM, Y. A.—HAYASHI, T.—YANAGISAWA, T.—MURAMATSU, H.—EZAKA, M.—TERRONES, H.—TERRONES, M.—DRESSELHAUS, M. S.: Carbon, *41*, 2003, p. 1941. doi:10.1016/S0008-6223(03)00171-4
[36] ZHAO, N. Q.—HE, C. N.—DING, J.—ZOU, T. C.—QIAO, Z. J.—SHI, C. S.—DU, X. W.—LI, J. J.—LI, Y. D.: J. Alloys Compd, *428*, 2007, p. 79. doi:10.1016/j.jallcom.2006.03.067
[37] EVANS, S.—THOMAS, J. M.: Proc. Roy. Soc., *353*, 1977, p. 103. doi:10.1098/rspa.1977.0024
[38] VAN ATTEKUM, P.—WERTHEIM, G. K.: Phys. Rev. Lett., *43*, 1979, p. 1896. doi:10.1103/PhysRevLett.43.1896
[39] LEIRO, J. A.—HEINONEN, M. H.—LAIHO, T.—BATIREV, I. G. J.: Electron. Spectrosc. Relat. Phenom., *128*, 2003, p. 205. doi:10.1016/S0368-2048(02)00284-0
[40] GALUSKA, A. A.—MADEN, H. H.—ALLRED, R. E.: Appl. Surf. Sci., *32*, 1988, p. 253. doi:10.1016/0169-4332(88)90012-8
[41] LASCOVICH, J. M.—GIORGI, R.—SCAGLIONE, S.: Appl. Surf. Sci., *47*, 1999, p. 17. doi:10.1016/0169-4332(91)90098-5
[42] JACKSON, S. T.—NUZZO, R.G.: Appl. Surf. Sci., *90*, 1995, p. 195. doi:10.1016/0169-4332(95)00079-8
[43] DRESSELHAUS, M. S.—DRESSELHAUS, G.—SAITO, R.—JORIO, A.: Physics Reports, *409*, 2005, p. 47. doi:10.1016/j.physrep.2004.10.006
[44] FERRARI, A. C.—ROBERTSON, J.: Phys. Rev., *64*, 2001, p. 075414.
[45] POCSIK, I.—HUNDHAUSEN, M.—KOOS, M.—LEY, L.: J. Non. Cryst. Solids, *230*, 1998, p. 1083.
[46] SOOD, A. K.—GUPTA, R.—ASHER, S.: J. Appl. Phys., *90*, 2001, p. 4494. doi:10.1063/1.1408590
[47] LI, X.—HAYASHI, J.—LI, C. Z.: Fuel, *85*, 2006, p. 1700.
[48] ZANG, Y.—TANG, Y. H.—LIN, L. W.—ZHANG, E. L.: Trans. Nonferrous Met. Soc., *18*, 2008, p. 1094.
[49] CHOI, S.—PARK, K. H.—HAN, J. H.—LEE, K. M.—LEE, S.—KOH, K. H.: J. Vac. Sci. Technol., *21*, 2003, p. 576. doi:10.1116/1.1527644
[50] PARK, K. H.—LEE, S.—KOH, K. H.: Diamond Rel. Mater., *14*, 2005, p. 2094.
[51] NATH, N.—SATISHKUMER, B. C.—COVINDARAJ, A.—VINOD, C. P.—RAO, C. N. R.: Chem. Phys. Lett., *322*, 2000, p. 333. doi:10.1016/S0009-2614(00)00437-1